Mechanistic Modeling of Marsh Seedling Establishment Provides a Positive Outlook for Coastal Wetland Restoration Under Global Climate Change

Zhan Hu[1,2,3] , **Bas W. Borsje[4]** , **Jim van Belzen[5]** , **Pim W. J. M. Willemsen[4]** , **Heng Wang[6]** , **Yisheng Peng[7]** , **Lin Yuan[8]**, **Michela De Dominicis[9]** , **Judith Wolf[9]** , **Stijn Temmerman[10]**, and **Tjeerd J. Bouma[5,11,12]**

[1]School of Marine Sciences, Sun Yat-Sen University, and Southern Marine Science and Engineering Guangdong Laboratory (Zhuhai), Zhuhai, China, [2]Guangdong Provincial Key Laboratory of Marine Resources and Coastal Engineering, Guangzhou, China, [3]Pearl River Estuary Marine Ecosystem Research Station, Ministry of Education, Zhuhai, China, [4]Water Engineering and Management, University of Twente, Enschede, The Netherlands, [5]Department of Estuarine and Delta Systems, Royal Netherlands Institute for Sea Research (NIOZ), Yerseke, The Netherlands, [6]National Engineering Laboratory for Port Hydraulic Construction Technology, Tianjin Research Institute for Water Transport Engineering, M.O.T, Tianjin, China, [7]School of Environmental Science and Engineering, Sun Yat-Sen University, Guangzhou, China, [8]State Key Laboratory of Estuarine and Coastal Research, Institute of Estuarine and Coastal Research, Institute of Eco-Chongming, East China Normal University, Shanghai, China, [9]National Oceanography Centre, Liverpool, UK, [10]Ecosystem Management Research Group, University of Antwerp, Wilrijk, Belgium, [11]Department of Physical Geography, Faculty of Geosciences, Utrecht University, Utrecht, The Netherlands, [12]Building with Nature group, HZ University of Applied Sciences, Vlissingen, The Netherlands

Abstract While many studies focus on the persistence of coastal wetlands under climate change, similar predictions are lacking for new wetland establishment, despite being critical to restoration. Recent experiments revealed that marsh seedling establishment is driven by a balance between physical disturbance of bed-level dynamics and seedling root stability. Using machine learning, we quantitatively translate such finding in a new biogeomorphic model to assess marsh establishment extent. This model was validated against multiyear observations of natural seedling-expansion events at typical sites in the Netherlands and China. Subsequently, synthetic modeling experiments underscored that seedling expansion was primarily determined by controllable local conditions (e.g., sediment supply, local wave height, and tidal flat bathymetry) rather than uncontrollable climate change factors (e.g., change in sea-level and global wave regime). Thus, science-based local management measures can facilitate coastal wetland restoration, despite global climate change, shedding hope for managing a variety of coastal ecosystems under similar stresses.

Plain Language Summary Vulnerability of coastal wetlands under climate changes is of global concern due to their valuable services. Thus, restoring coastal wetlands is of widespread importance. However, the key processes controlling wetland vegetation establishment are not clear until recent field and laboratory experiments using marshes as an exemplary system. In the current study, we translate the insights of these recent studies into a new biogeomorphic model to predict marsh establishment extent on a landscape scale. Synthetical model analysis underlines that controllable local conditions are much more important than uncontrollable climate change stressors, thus providing a positive outlook for future coastal wetland restorations.

1. Introduction

Coastal biogeomorphic systems are among the most valuable (Barbier et al., 2008; Borsje et al., 2011), but also most vulnerable ecosystems around the globe (Brown et al., 2014; Friess et al., 2019; Parkinson et al., 2017). Tidal marshes are exemplary for these ecosystems, in providing highly valued ecosystem services, such as carbon storage (Kirwan & Mudd, 2012; Mcleod et al., 2011) and flood risk mitigation (Arkema et al., 2015; Smith et al., 2016; Temmerman et al., 2013; van Loon-Steensma et al., 2016; Zhu et al., 2020), while also being prominently affected by global climate change. Global-scale projections suggest that a relative sea-level rise (RSLR) alone can lead to 20%–90% loss of the current marsh areas by 2100 (Kirwan,

Temmerman, et al., 2016; Schuerch et al., 2018; Thorne et al., 2018). Such loss may be further exacerbated by increased storminess (Young et al., 2011), global significant wave height rise (HsR) (Young & Ribal, 2019), and reduced sediment supply to the coasts (Ganju et al., 2017; Ladd et al., 2019). While previous studies have advanced the assessment of the loss and retreat of existing marshes (D'Alpaos et al., 2007; Leonardi et al., 2015), further efforts are need to provide science-based strategies to (re)create new marshes and counteract the impacts of global climate change.

Seedling establishment is a key process for marsh (e.g., *Spartina spp.*) creation in many coastal and estuarine areas around the world (Ayres et al., 2008; Balke et al., 2016), which can drive rapid recruitment over extensive intertidal areas (Gray et al., 1991; Strong & Ayres, 2013, see also Figure S1 in Supporting Information S1). These establishment events are particularly relevant in areas that are disconnected from existing vegetation patches, e.g., in front of marsh cliffs or at unvegetated restoration sites. Seedling establishment is typically followed by clonal growth that eventually merges scattered vegetation patches into contiguous canopies (van der Wal et al., 2008; Zhu et al., 2012). Therefore, seedling establishment is a key process determining restoration potentials. Mechanistic modeling of such a process can provide insights needed for restoration practices. However, seedling establishment events are episodic rather than gradual due to the dynamic nature of intertidal bed level, which is difficult to predict. Our current modeling ability of marsh establishment extent is inadequate, as marsh extent is generally assessed by empirical relations considering intertidal elevation (Ge et al., 2016; Wang & Temmerman, 2013) or hydrodynamic forcing (Hu, Van Belzen, et al., 2015; Schwarz et al., 2018).

In intertidal environments, marsh seedlings are frequently disturbed by periodic inundation, currents, waves, and the resulting bed-level dynamics (i.e., sediment erosion and deposition) (Callaghan et al., 2010; D'Alpaos et al., 2013). Successful establishment in such systems requires sequences of low-disturbance periods directly following seed dispersal. These critical sequences of periods are referred to as windows of opportunity, during which seedlings gain their initial stability by root anchorage (Balke et al., 2014; Hu, Van Belzen, et al., 2015). Windows of opportunity are composed of (a) an initial inundation-free period (a few days) and (b) a subsequent period when the physical disturbance is within seedlings tolerance (a few weeks). Recent field and laboratory experiments have revealed that the balance between short-term bed-level dynamics (as external disturbance) and seedling root growth (as internal tolerance) in the second period determines whether seedlings are uprooted and lost or able to grow up into mature plants (Bouma et al., 2016; Cao et al., 2018, Figure 1). The role of this critical antagonistic relationship has not yet been included in the existing marsh dynamic models. Proper incorporation of such key insight provides an opportunity to mechanistically model seedling establishment process and the impact of environmental changes, for example, RSLR (Syvitski et al., 2009), changing wave regime (Young & Ribal, 2019; Young et al., 2011), and sediment starvation (Ganju et al., 2017; Ladd et al., 2019).

Using machine learning, we translated the insights and data from recent experiments into a new biogeomorphic model to predict windows of opportunity for marsh seedling establishment. With this model, we aim to reveal the key stressors limiting marsh establishment and identify effective local restoration measures. We first validated the model by accurately simulating the presence and absence of seedling expansion events over multiple years at two typical sites in the Netherlands and in China. Subsequently, we used the validated model to assess seedling expansion in various scenarios of global climate change (i.e., RSLR, increased storminess, and HsR) and local management measures (i.e., sediment supply, implementing wave damping structures, and sediment nourishment).

2. Materials and Methods

2.1. General Description of Model Approach

A new biogeomorphic model was developed based on a previous windows of opportunity model (Hu, Van Belzen, et al., 2015) to predict the spatiotemporal occurrence of marsh seedling establishment (Figure 1). The previous model considers that successful establishment requires a sufficiently long inundation-free period (e.g., 3 days) and a subsequent period when time-dependent bed shear stress needs to remain below calibrated critical values. The novelty of the current model lies in the quantitative representation of the
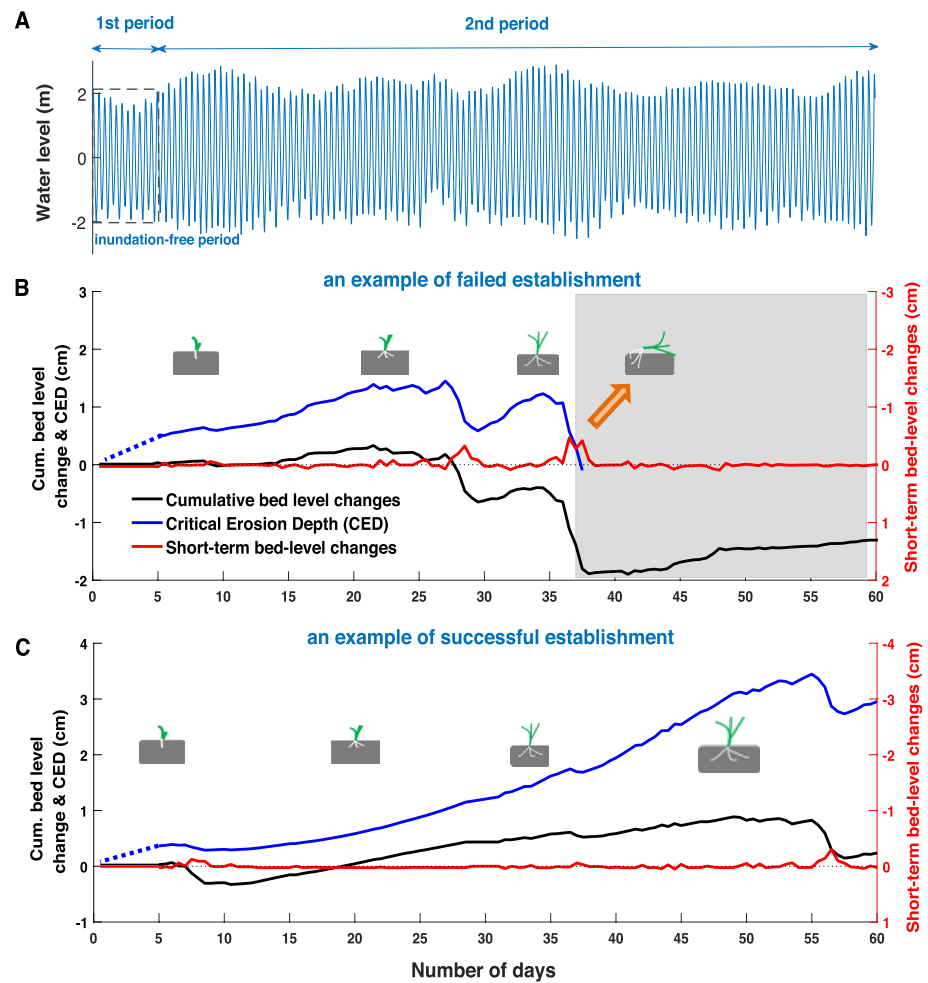
Figure 1. A general introduction to the seedling establishment model. (a) A window of opportunity is composed of a first period free of inundation and a second period when the physical disturbance of bed-level dynamics is within seedlings tolerance. (b) An example of failed seedling establishment, in which the short-term bed erosion exceeds the seedling tolerance (Critical Erosion Depth, [CED]) around 37th day (i.e., when the red line intersects the blue line). CED varies consistently with cumulative bed-level changes over time as net accretion enhances root anchorage and net erosion impairs it. For both cumulative and short-term bed-level changes, positive values indicate accretion and negative values indicate erosion, but the values on the Y axis are inversed. (c) An example of successful seedling establishment, in which the short-term erosion is always below CED, that is., within seedlings tolerance.

driving processes in seedling establishment in the second period (i.e., the balance between seedling root growth and magnitude of bed-level changes), avoiding the inclusion of latent factors.

Based on the results of recent field and mesocosm experiments (Bouma et al., 2016; Cao et al., 2018), successful establishment via windows of opportunity requires: (a) an initial inundation-free period (several days) directly following seed dispersal to allow for germination and (b) a subsequent period (several weeks) with low bed-level dynamics to sufficiently achieve deep root anchorage (Figure 1). Marsh seedling survival in the second period is determined by the antagonistic relationship between physical disturbance (i.e., daily bed erosion or sedimentation) and temporal development of seedling resistance (i.e., increase of root depth). Seedling tolerance to bed erosion is quantified as the Critical Erosion Depth (CED). Successful establishment requires short-term bed erosion (over one tidal cycle) to be always lower than the CED. If erosion exceeds CED at any moment during the second period, then seedlings will be dislodged from the bed, impeding the establishment (Figure 1b). We assume that seedlings can successfully establish if they live through the second period. In reality, they can still be dislodged from the bed if the subsequent bed

erosion is too high. However, the most critical period determining seedling establishment would be the first few weeks in the windows of opportunity when the root anchorage is not deep enough.

Experiments have shown that CED varies over time (Bouma et al., 2016; Cao et al., 2018). It is internally influenced by seedling root growth, which increases CED, and externally by cumulative bed-level changes, i.e., net accretion increases the CED and net erosion decreases the CED (Figures 1b and 1c). In our model, we used a machine-learning technique (Artificial Neural Networks) to translate recent experimental data into two CED predictors for both *S. anglica* and *S. alterniflora* seedlings, respectively (Hu, 2021). They give predictions of CED for each tidal cycle after the initial inundation-free period. We identified three parameters as inputs of these predictors: (a) the duration of the initial inundation-free period, (b) the survival time in the second period before seedlings are killed or toppled by too much erosion, and (c) the cumulative bed-level changes during the second period. The procedure of training and testing the machine-learning predictors is described in more detail in Text S1 in Supporting Information S1. Seedling tolerance to sediment accretion is quantified as MAR (Maximum Accretion Rate) based on the experiments in Cao et al. (2018). For *S. anglica* seedlings, MAR is set as a net accretion of 1.8 cm in one week or 2.4 cm in two weeks. For *S. alterniflora* seedlings, MAR is set as a net accretion of 1.2 cm in one week.

Bed-level change in biogeomorphic model was provided by the DET-ESTMORF model (Hu, Wang, et al., 2015), which implements the dynamic equilibrium theory (DET) by Friedrichs (2011). It explicitly accounts for deviation between the uniform bed shear stress (associated with tidal flat equilibrium) and the actual bed shear stress from tidal currents and wind waves to predict tidal flat morphodynamics. The model has shown good agreement with other models (Liu et al., 2011; Maan et al., 2015; Roberts et al., 2000) and field observations (Hu, Wang, et al., 2015), thus providing a good base to support the current biogeomorphic modeling. In this study, it has been quantitatively validated at transect P25 at Western Scheldt site and qualitatively tested at the Yangtze Estuary site (Figure 2). DET-ESTMORF model input and validation are described in Text S2 in Supporting Information S1.

2.2. Observation of Seedling Expansion and Model Setting at Two Study Sites

Seedling occurrence at our two sites was observed at a spatial resolution of 1 m to generate a data matrix for model validation (Figure 2e). At the Western Scheldt site, the pioneer species is *S. anglica*. The spatiotemporal occurrence of seedling establishment was obtained on 4 cross-shore profiles (P20, P25, P50, and P70) during 2004–2012 by using aerial photographs from Dutch Department of Public Works and Water Management. At the Yangtze Estuary site, seedling occurrence of *S. alterniflora* was obtained from georeferenced Landsat-5 TM images (2008) and Formasat-2 images (2011). The remote sensing observation was complemented by published field survey data at 1-m resolution collected during 2009–2012 (Cao et al., 2014; Ge et al., 2013).

The obtained seedling observation matrix was used to test model performance. In our model, seedling growing season was set as 1st April–1st October (Balke et al., 2014). The minimum duration of the initial inundation-free period was set as 3 days (Balke et al., 2014). The duration of the second period was the only unknown parameter requiring calibration for the inclusion of the balance between seedling root growth and magnitude of bed-level changes. Other parameters were adapted from the original morphodynamic model (Hu, Wang, et al., 2015), and the CEDs of the different species at two sites were automatically quantified by machine-learning predictors, which do not require calibration. Sensitivity analysis showed that model accuracy is insensitive to variation in the duration of the second period (5–12 weeks, Table S1 in Supporting Information S1). The second period was then set as 8 weeks to reach the best agreement with the observations. To avoid inflating model accuracy, our model assessment was only conducted on bare flat areas that were high enough for potential marsh establishment (higher than 0.6 m below mean high water level) (Wang & Temmerman, 2013). The areas that were too low to accommodate establishment were excluded from seedling occurrence assessment but still included in the morphodynamic modeling.

2.3. Scenarios of Climate Change and Protective Management Measures

To assess the impact of climate change and local conditions on extent of seedling establishment, model experiments of various scenarios were conducted (Table 1). We define the most seaward location with
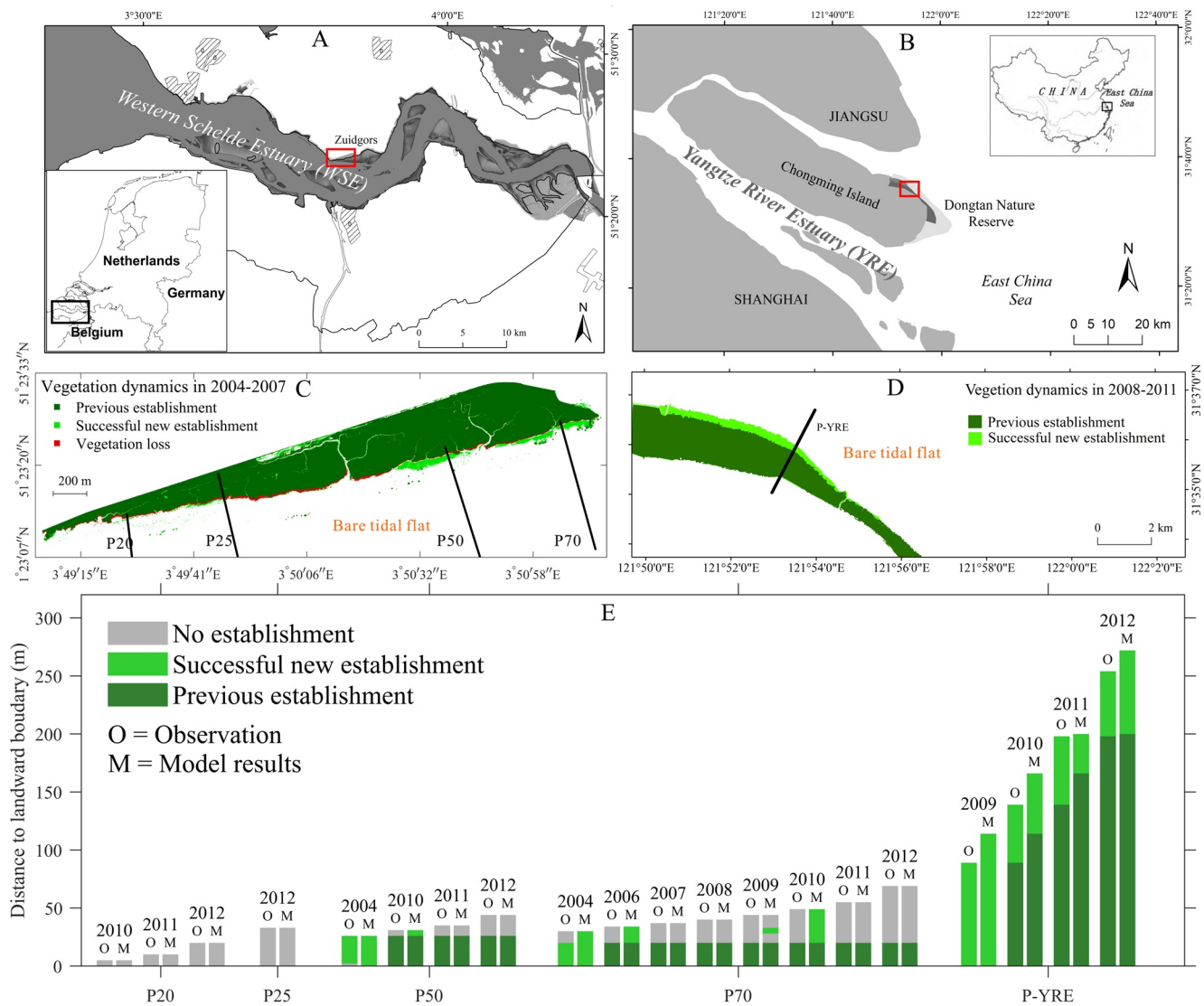
Figure 2. Observed and modeled marsh seedling establishment extent at two sites. (a) The Westerschelde Estuary site, the Netherlands. (b) The Yangtze Estuary site, China. (c) Remotely sensed vegetation cover dynamics in 2004–2012 at the Westerschelde Estuary site with 4 monitoring profiles: p20, p25, p50, and p70. (d) Remotely sensed vegetation cover dynamics in 2008–2011 at the Yangtze Estuary site. (e) Comparison between observed and modeled marsh seedling establishment occurrence at both sites. The "No establishment" areas are the areas with sufficiently high elevation (above the mean high water level-0.6 m) (Wang & Temmerman, 2013) but no seedling establishment.

windows of opportunity for establishment as the pioneer marsh edge (Hu, Van Belzen, et al., 2015). By tracking the position of the seaward marsh edge, we estimated changes in pioneer marsh width in various scenarios. For comparison, all these changes were referenced to the initial marsh width (after first year) on an equilibrium profile in the base run (see Figure 3). The equilibrium profile was obtained by 100-year morphodynamic modeling (without marsh establishment modeling) starting from a linear profile, after which bed-level changes were negligible. This results in a typical bare flat that is close to natural conditions when a restoration project starts, on which we performed the marsh establishment modeling in different scenarios. The prediction was conducted over a decadal time span, as it is the typical duration for marsh restoration projects (Adam, 2019; Currin et al., 2017). To obtain the equilibrium profile, the mean tidal range (with spring-neap tides), mean wave height, and Suspended Sediment Concentration (SSC) at model boundary were set as 4.2 m, 0.22 m, and 80 mg/L, respectively. These settings were chosen to obtain a reference profile with sufficient space for profile expansion and retreat in different scenarios (see Figure 3). In different scenarios, the profiles do not necessarily reach equilibrium over the decadal modeling period.

Table 1
Impact of Global Stressors and Local Conditions on Marsh Seedling Establishment and Available Management Options

Stressor type	Variable	Range	Impact	Management options
Global stressors[a]	RSLR	0–30 mm/yr (Syvitski et al., 2009)	Low	-
	Rise in significant wave height (HsR)	0–10 mm/yr (Young & Ribal, 2019)	High	Wave damping structures, e.g., oyster reefs (Chowdhury et al., 2019; de Paiva et al., 2018) and brushwood dams (Borsje et al., 2017)
	Rise in storm intensity	0%–2%/yr (Young et al., 2011)	Low	-
	Rise in storm frequency	0%–2%/yr (Young et al., 2011)	Low	-
Local conditions[b]	Sediment supply	10–150 mg/l (Kirwan, Walters, et al., 2016)	High	Increase sediment supply by opening upstream dam or creating river diversions (Giosan et al., 2014; Mariotti & Fagherazzi, 2013; Nittrouer et al., 2012)
	Significant wave height	−10–10 mm/yr (Borsje et al., 2017; Chowdhury et al., 2019; van Loon-Steensma et al., 2016; de Paiva et al., 2018)	High	Wave damping structures, e.g., oyster reefs (Chowdhury et al., 2019; de Paiva et al., 2018) and brushwood dams (Borsje et al., 2017)
	Tidal flat profile shape	concave, equilibrium, and convex profiles (Friedrichs, 2011)	High	Sediment nourishment (Baptist et al., 2019; van der Werf et al., 2015)

[a]These stressors are the consequences of global climate change, but their specific magnitude varies regionally over distances larger than 10^2–10^3 km. [b]Local conditions may vary over distances of just a few 100 meters.

The tested RSLR varied from 0 to 30 mm/yr (Syvitski et al., 2009). The maximum value corresponds to areas with fast land subsidence, for example, Yangtze Estuary. To explore the effects of changing wave climate on seedling establishment, we varied significant wave height (HsR), storm intensity, and frequency. Variations in significant wave height were achieved by adding a positive or negative changing rate to the original time series. Negative HsR values mimic the situations with local wave-damping structures, for example, oyster reefs (Chowdhury et al., 2019; de Paiva et al., 2018) and brushwood dams (Borsje et al., 2017). In contrast to HsR, which may directly respond to local interventions, changes in storm frequency and intensity (0%–2% per year, Table 1) are assumed to be solely driven by global wave climate change (Young et al., 2011).

To reveal the impact of sediment supply, boundary SSC varied from 10 to 150 mg/l (Kirwan, Walters, et al., 2016). The neutral sediment condition was the SSC that led to the original equilibrium profile, that is, 80 mg/l, whereas the sediment deficit and surplus conditions were then the SSC below or above the neutral sediment level. To explore the effect of intertidal profile shape on seedling establishment, we conducted model experiments on concave, equilibrium, and convex profiles. The concave profile exemplifies tidal flats that are suffering from sediment starvation and/or channel dredging (Friedrichs, 2011), whereas the equilibrium profile represents natural stable tidal flats, and the convex profile represents tidal flats with sediment-nourishment (Baptist et al., 2019; van der Werf et al., 2015). The initially concave and convex profiles were created following Hu, Van Belzen, et al. (2015).

3. Results

3.1. Natural Seedling Establishment at Two Sites With Different Sediment Supply

Observations via remote sensing and supplementary field surveys have revealed different seedling establishment occurrences at the two study sites in the Netherlands and in China (Figures 2c and 2d). The Western Scheldt Estuary site has relatively stable intertidal flats and marshes, where seedling (*S. anglica*) establishment in front of the mature marsh has only occurred episodically in 2004 on two out of four monitored profiles. In the following period (2005–2012), no new expansion occurred on any of the profiles. In contrast, the Yangtze Estuary site had continuous seedling (*S. alterniflora*) establishment on a seaward-expanding intertidal flat over the period of 2009–2012 (Figures 2e and S3 in Supporting Information S1).

Our mechanistic modeling approach is able to accurately reproduce the presence and absence of seeding establishment events observed at both sites (Figure 2e). The accuracy of the prediction is 81% for the Western
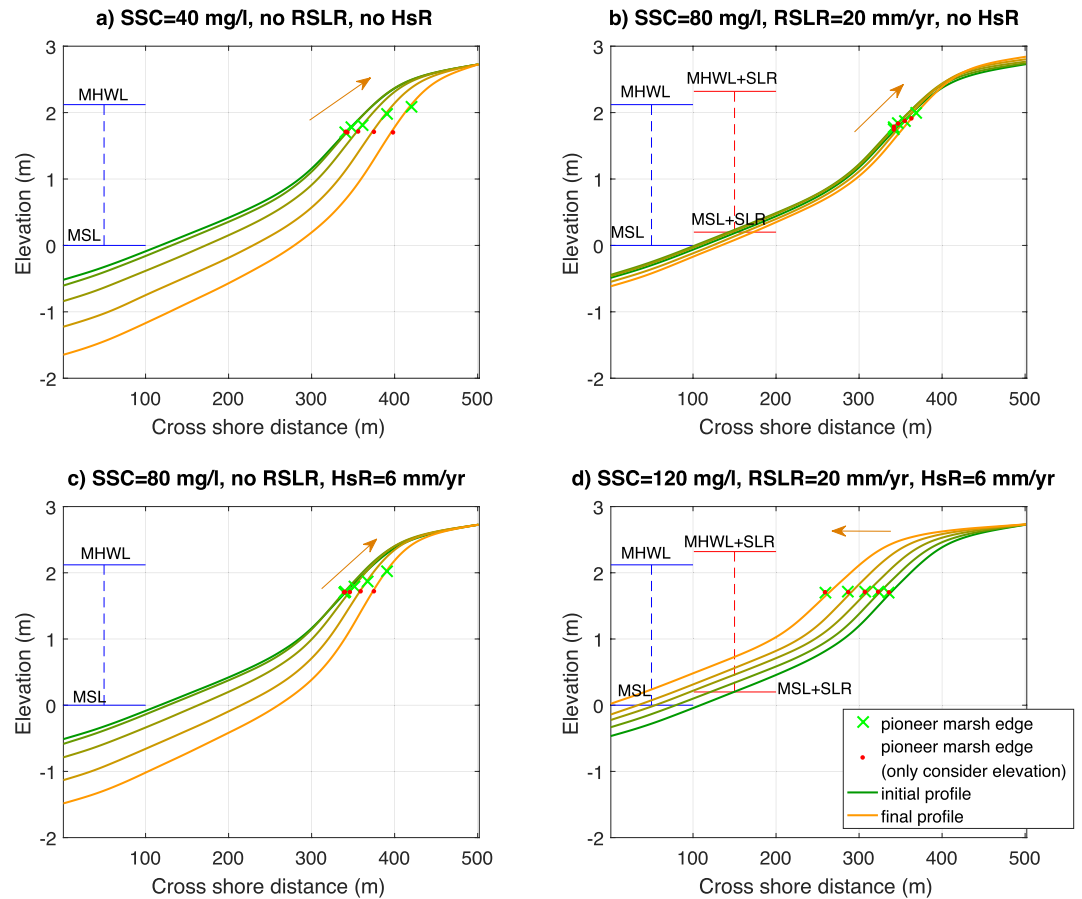
Figure 3. Decadal tidal flat profile evolution and changes in pioneer marsh edge based on an initial equilibrium profile (described in Section 2.3). (a) Scenario with no climate changes (no relative sea level rise [RSLR] nor HsR), but with low sediment supply, that is, Suspended Sediment Concentration (SSC) is 40 mg/l. (b) Scenario with RSLR and neutral sediment supply, that is, SSC is 80 mg/l. (c) Scenario with HsR and neutral sediment supply. (d) Scenario with both RSLR and HsR, but with high sediment supply, that is, SSC is 120 mg/l. Green crosses indicate the predicted pioneer marsh edge of the current model, whereas red dots indicate the predicted pioneer marsh edge only considering elevation, i.e., the first period in windows of opportunity. Arrows indicate the direction of marsh edge movement. Positive HsR mimics a rise in significant wave height due to global wave regimen change.

Scheldt Estuary site and 75% for the Yangtze Estuary site. The duration of the second period in windows of opportunity is the only parameter that needs calibration. The model accuracy does not significantly vary during calibration (Table S2 in Supporting Information S1), showing the robustness of the model. In particular, potential areas for new establishment with high enough elevations emerged after 2004 at the Western Scheldt Estuary site (Figure S2 in Supporting Information S1). In such case, previous models that assess establishment solely based on elevation would overestimate the extent of marsh expansion. Our model, however, correctly captures the episodic seedling establishment events occurred in 2004 and the absence of such events afterward with few errors.

The model results further reveal that the distinctive seedling establishment patterns between the two sites, being episodic at the Western Scheldt Estuary site versus quasi-continuous at the Yangtze Estuary site, are likely induced by the differences in sediment supply. SSC at the Yangtze Estuary site (210–880 mg/l) (Li et al., 2012) is much higher than that at the Western Scheldt Estuary site (31–71 mg/l) (Hu et al., 2018). The higher SSC leads to continuous sediment accretion over both short term (Figure S4 in Supporting Information S1) and long term (Figure S3 in Supporting Information S1), which facilitates continuous seedling establishment. This distinctive establishment pattern cannot be explained by the difference in marsh species since the tolerances of these two species to bed-level changes are similar (Figure S5 in Supporting Information S1). This contrast was not caused by differences in hydrodynamic conditions either, as the Western

Scheldt site actually has a larger tidal range (4.10 vs. 2.69 m) and smaller incident waves (mean significant wave height 0.12 vs. 0.42 m) than the Yangtze Estuary site (Dai et al., 2016), which would suggest more frequent and extensive marsh expansion (Balke et al., 2016; Hu, Van Belzen, et al., 2015). Since the opposite is true, sediment supply is potentially the primary driver of the observed seedling establishment patterns.

3.2. Combined Effect of Global Stressors and Local Measures

The validated model was subsequently used to predict seedling establishment extent in various scenarios of global climate change (RSLR and HsR) and local sediment supply (Figure 3). We started with *S. anglica* establishing on a schematized equilibrium tidal flat, which was built with SSC = 80 mg/L (see Section 2.3). The results show that in case of sediment deficit (40 mg/L), even without the impacts of RSLR nor HsR, the tidal flat erodes continuously as previous equilibrium with adequate sediment supply (80 mg/L) is broken (Figure 3a). Our model predicts that in such a case, pioneer marsh is forced to retreat to a higher elevation (up to ca. 0.4 m) and more landward locations comparing to the modeling results that only consider elevation. Such difference shows the importance of considering bed-level dynamics in the modeling. The retreat is expected to continue after the decade until a new equilibrium is reached. In case of RSLR (20 mm/yr) and neutral sediment supply level, tidal flat profile is only slightly steepened. The pioneer marsh edge is driven to higher locations, but the change in pioneer marsh area is small (Figure 3b). The test with positive HsR (6 mm/yr) gives similar prediction as the test with low sediment input, that is, strongly eroded tidal flats with retreated pioneer marsh (Figure 3c). Notably, the test with sufficient sediment inputs (SSC = 120 mg/L) shows that pioneer marsh width can expand with tidal flats accretion, despite the impacts of HsR and RSLR (Figure 3d). Such expansion may continue with the profile progradation until a new equilibrium is established. In such a case, our model derives similar results as the models that only consider elevation.

Next, we synthetically model the dynamics of pioneer marsh width under the combined effects of global climate change and local conditions, including sediment supply, local wave height, and intertidal profile shape (Figure 4). In scenarios with combined effect of RSLR and varying sediment supply, the impact of the former is much weaker than the latter: sufficient sediment supply leads to pioneer marsh expansion, whereas insufficient sediment supply leads to retreat (Figure 4a). RSLR merely aggravates marsh retreat in case of low sediment inputs. In contrast, tests with combined effect of HsR and sediment supply show that both factors jointly determine the rate of marsh expansion or retreat (Figure 4b). Pioneer marsh shrinks with positive HsR, but expands with negative HsR, which can be achieved by implementing wave-damping structures. Comparing to HsR, increases in storm frequency and intensity show a limited impact on pioneer marsh width (Figure S6 in Supporting Information S1).

Lastly, our model reveals striking differences of marsh establishment on concave, equilibrium, and convex profiles. We used these profiles to exemplify eroded, natural, and sediment-nourished tidal flats as concave-up and convex-up profiles are often associated with net sediment erosion and accretion, respectively (Friedrichs, 2011). Under the same condition, marsh expansion is far more likely on a convex profile than on equilibrium or concave profiles (Figures 4d–4f). Marsh contraction is common on concave profiles, where seedling expansion is only possible when both sediment input is high and HsR is negative (Figure 4d). The apparent difference can be attributed to the fact that convex profiles have wider elevated areas to host seedling (Wang & Temmerman, 2013) and even more importantly have greater ability in attenuating incident waves to reduce short-term sediment erosion (Currin et al., 2017; Hu, Van Belzen, et al., 2015).

4. Conclusions and an Outlook for Coastal Wetlands Restoration

An overview of various stressors and corresponding management options is given in Table 1. It is not surprising that the RSLR does not have a large effect as the considered decadal time span is short. In contrast, the impact of HsR is much more important for restoration projects over the same time span. While previous studies have identified the key impact of wave height on mature marsh width (Leonardi et al., 2015; Marani et al., 2011), our results show that it is also critical in determining pioneer marsh extent. A rise in mean wave height is expected in many parts of the world (Young & Ribal, 2019), which threats new marsh establishment. Building local wave-damping structures, such as oyster reefs (Chowdhury et al., 2019; de Paiva
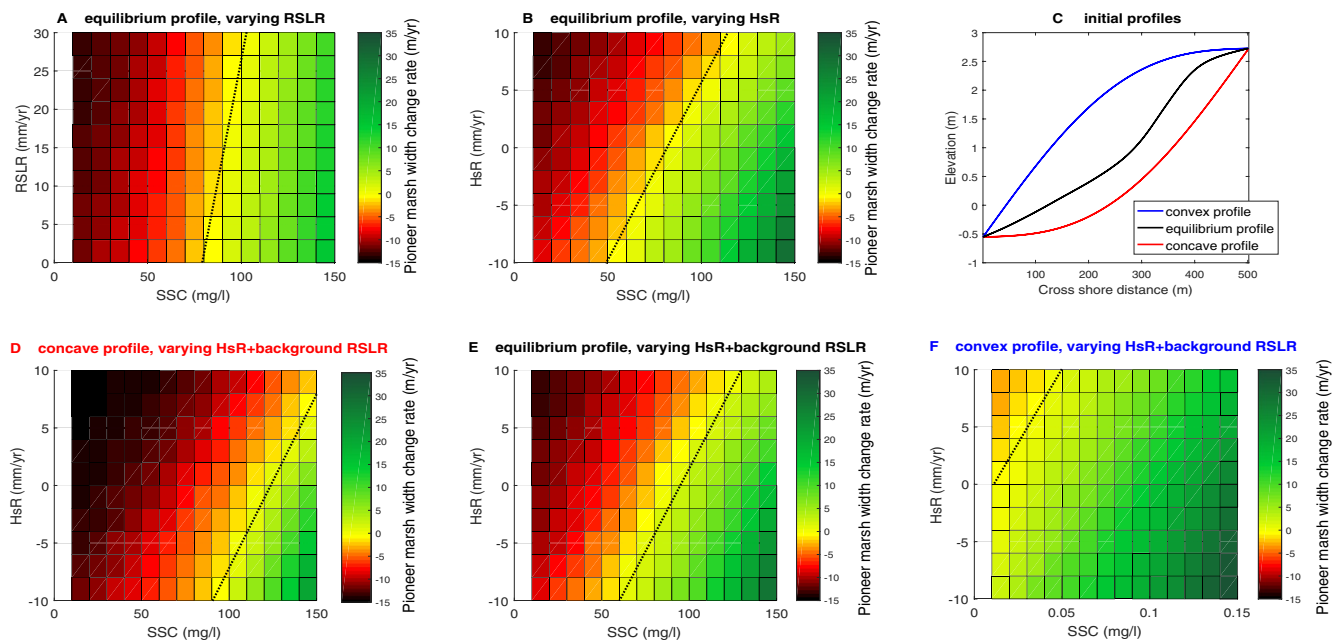
Figure 4. Phase diagrams illustrating the change rate of pioneer marsh width (seedling establishment extent) with climate change stressors and management measures over decadal time span. All the changes were referenced to the pioneer marsh width on equilibrium profiles (i.e., initial profiles in Figure 3). (a) Scenarios with different sediment supply levels (SSC = 10–150 mg/l) and varying relative sea-level rise (RSLR) speed (0–30 mm/yr). (b) Scenarios with different sediment supply levels and varying HsR rates (−10 to 10 mm/yr), based on an initial equilibrium profile. The positive HsR mimics a rise in mean wave height due to global wave regime change, whereas the negative HsR mimics cases with local wave-damping structures, e.g., brushwood dams. (c) Initial concave, equilibrium, and convex profiles used in the model, which exemplify eroded, stable, and accreting (e.g., nourished) tidal flats, respectively. (d–f) Tests with initial concave, equilibrium, and convex profile shapes and varying sediment supply levels, HsR rate, and a background RSLR = 20 mm/yr. Black-dotted lines indicate the cases with width change rates close to zero.

et al., 2018) and permeable brushwood dams (Borsje et al., 2017), can generate favorable local wave climate for restoration.

We highlight that sufficient sediment supply is necessary in creating new accommodation area for marsh expansion (Mariotti & Canestrelli, 2017) and in mitigating short-term erosion to facilitate seedling establishment (Table 1 and Figure S4 in Supporting Information S1). Successful marsh restoration projects may request temporarily opening upstream river dams or creating river diversions to direct sediment-rich water into managed marsh systems (Mariotti & Fagherazzi, 2013; Nittrouer et al., 2012). When these watershed-scale operations are not feasible, local sediment-nourishment operations that increase tidal flat convexity can be considered to accommodate seedling establishment (Baptist et al., 2019; van der Werf et al., 2015). Unlike sandy beaches, where nourishment is a common practice (Stive et al., 2013), nourishing muddy tidal flats using dredged sediment remains relatively unexplored. In countries like the UK, such practice faces complex regulations, and dredged sediment remains an underused resource (Ausden et al., 2016). Our study suggests that a wider application of sediment nourishment can greatly benefit marsh restoration.

The newly developed model opens up new venues for the assessment of marsh seedling establishment. It can also form a component for long-term cyclic marsh dynamics modeling, including both expansion phases (characterized by seedling establishment) and retreat phases (characterized by cliff lateral erosion) (Allen, 2000; Singh Chauhan, 2009). The current model can be applied to assess seedling establishment on bare flat or reestablishment in front of retreating cliffs. The latter is the key process that reverse marsh retreat to new expansion (Bouma et al., 2016). However, cyclic marsh dynamics is more apparent in macrotidal systems. In microtidal systems, marsh expansion is primarily though clonal growth rather than seedling establishment, where our model applicability is restrained.

Similar to marshes, a number of coastal biogeomorphic systems have to establish via windows of opportunity in physical dominated environments, for example, mangroves (Balke et al., 2011; Bryan et al., 2017)

and seagrass meadows (Suykerbuyk et al., 2015). Importantly, our results provide a positive outlook for coastal restoration in the era of global climate change. Local conditions that can be controlled by management measures (i.e., sediment supply, local wave height, and tidal flat profiles) have a greater influence on marsh seedling expansion than uncontrollable climate change stressors (i.e., RSLR and global wave regime). Thus, well-conceived local measures can still create opportunities for successful restorations, despite climate change.

Data Availability Statement

Marsh seedling establishment data, model output, and the model code for the machine-learning predictors are available from Zenodo at https://doi.org/10.5281/zenodo.4916905. The morphodynamic model (DET-ESTMORF) and the parameter settings are adapted from Hu, Wang, et al. (2015). The Critical Erosion Depth data of marsh seedlings are available in Bouma et al. (2016) and Cao et al. (2018). The bathymetry and hydrodynamics data at Western Scheldt site are available in Callaghan et al. (2010) and Hu, Van Belzen, et al. (2015). The bathymetry data at Yangtze Estuary site are available in Wang et al. (2014). The tidal range and suspended sediment concentration data at this site are available in Dai et al., (2016) and Li et al. (2012), respectively.

References

Adam, P. (2019). Chapter 23-Salt Marsh Restoration. In G. M. E. Perillo, E. Wolanski, D. R. Cahoon, & C. S. Hopkinson (Eds.), *Coastal wetlands* (pp. 817–861). Elsevier. https://doi.org/10.1016/B978-0-444-63893-9.00023-X

Allen, J. R. L. (2000). Morphodynamics of Holocene salt marshes: A review sketch from the Atlantic and Southern North Sea coasts of Europe. *Quaternary Science Reviews*, *19*(12), 1155–1231. https://doi.org/10.1016/s0277-3791(99)00034-7

Arkema, K. K., Verutes, G. M., Wood, S. A., Clarke-Samuels, C., Rosado, S., Canto, M., et al. (2015). Embedding ecosystem services in coastal planning leads to better outcomes for people and nature. *Proceedings of the National Academy of Sciences of the United States of America*, *112*(24), 7390–7395. https://doi.org/10.1073/pnas.1406483112

Ausden, M., Dixon, M., Lock, L., Richardson, N., & Scott, C. (2016). Dredged sediment–Still an under-used conservation resource. *British Wildlife*, *28*, 88–96.

Ayres, D. R., Zaremba, K., Sloop, C. M., & Strong, D. R. (2008). Sexual reproduction of cordgrass hybrids (Spartina foliosa × alterniflora) invading tidal marshes in San Francisco Bay. *Diversity and Distributions*, *14*(2), 187–195. https://doi.org/10.1111/j.1472-4642.2007.00414.x

Balke, T., Bouma, T. J., Horstman, E. M., Webb, E. L., Erftemeijer, P. L. A., & Herman, P. M. J. (2011). Windows of opportunity: Thresholds to mangrove seedling establishment on tidal flats. *Marine Ecology Progress Series*, *440*, 1–9. https://doi.org/10.3354/meps09364

Balke, T., Herman, P. M. J., & Bouma, T. J. (2014). Critical transitions in disturbance-driven ecosystems: Identifying windows of opportunity for recovery. *Journal of Ecology*, *102*(3), 700–708. https://doi.org/10.1111/1365-2745.12241

Balke, T., Stock, M., Jensen, K., Bouma, T. J., & Kleyer, M. (2016). A global analysis of the seaward salt marsh extent: The importance of tidal range. *Water Resources Research*, *52*(5), 3775–3786. https://doi.org/10.1002/2015WR018318

Baptist, M. J., Gerkema, T., van Prooijen, B. C., van Maren, D. S., van Regteren, M., Schulz, K., et al. (2019). Beneficial use of dredged sediment to enhance salt marsh development by applying a "Mud Motor. *Ecological Engineering*, *127*, 312–323. https://doi.org/10.1016/j.ecoleng.2018.11.019

Barbier, E. B., Koch, E. W., Silliman, B. R., Hacker, S. D., Wolanski, E., Primavera, J., et al. (2008). Coastal ecosystem-based management with nonlinear ecological functions and values. *Science*, *319*(5861), 321–323. https://doi.org/10.1126/science.1150349

Borsje, B. W., de Vries, S., Janssen, S. K. H., Luijendijk, A. P., & Vuik, V. (2017). Building with nature as coastal protection strategy in the Netherlands. In D. M. Bilkovic, M. M. Mitchell, M. K. La Peyre, & J. D. Toft (Eds.), *Living shorelines: The science and management of nature-based coastal protection* (pp. 137–156). CRC Press. https://doi.org/10.1201/9781315151465-10

Borsje, B. W., van Wesenbeeck, B. K., Dekker, F., Paalvast, P., Bouma, T. J., van Katwijk, M. M., & de Vries, M. B. (2011). How ecological engineering can serve in coastal protection. *Ecological Engineering*, *37*(2), 113–122. https://doi.org/10.1016/j.ecoleng.2010.11.027

Bouma, T. J., van Belzen, J., Balke, T., van Dalen, J., Klaassen, P., Hartog, A. M., et al. (2016). Short-term mudflat dynamics drive long-term cyclic salt marsh dynamics. *Limnology & Oceanography*, *61*(6), 2261–2275. https://doi.org/10.1002/lno.10374

Brown, C. J., Saunders, M. I., Possingham, H. P., & Richardson, A. J. (2014). Interactions between global and local stressors of ecosystems determine management effectiveness in cumulative impact mapping. *Diversity and Distributions*, *20*(5), 538–546. https://doi.org/10.1111/ddi.12159

Bryan, K. R., Nardin, W., Mullarney, J. C., & Fagherazzi, S. (2017). The role of cross-shore tidal dynamics in controlling intertidal sediment exchange in mangroves in Cù Lao Dung, Vietnam. *Continental Shelf Research*, *147*, 128–143. https://doi.org/10.1016/j.csr.2017.06.014

Callaghan, D. P., Bouma, T. J., Klaassen, P., van der Wal, D., Stive, M. J. F., & Herman, P. M. J. (2010). Hydrodynamic forcing on salt-marsh development: Distinguishing the relative importance of waves and tidal flows. *Estuarine, Coastal and Shelf Science*, *89*(1), 73–88. https://doi.org/10.1016/j.ecss.2010.05.013

Cao, H., Ge, Z., Zhu, Z., & Zhang, L. (2014). The expansion pattern of saltmarshes at Chongming Dongtan and its underlying mechanism. *Acta Ecologica Sinica*, *34*(14), 3944–3952. https://doi.org/10.5846/stxb201304110677

Cao, H., Zhu, Z., Balke, T., Zhang, L., & Bouma, T. J. (2018). Effects of sediment disturbance regimes on Spartina seedling establishment: Implications for salt marsh creation and restoration. *Limnology & Oceanography*, *63*(2), 647–659. https://doi.org/10.1002/lno.10657

Chowdhury, M. S. N., Walles, B., Sharifuzzaman, S. M., Hossain, M. S., Ysebaert, T., & Smaal, A. C. (2019). Oyster breakwater reefs promote adjacent mudflat stability and salt marsh growth in a monsoon dominated subtropical coast. *Scientific Reports*, *9*(1), 1–12. https://doi.org/10.1038/s41598-019-44925-6

Currin, C. A., Davis, J., & Malhotra, A. (2017). Response of Salt Marshes to Wave energy provides Guidance for Successful Living Shoreline Implementation. In D. M. Bilkovic, M. M. Mitchell, M. K. La Peyre, & J. D. Toft (Eds.), *Living shorelines: The science and management of nature-based coastal protection* (pp. 209–232). CRC Press. https://doi.org/10.1201/9781315151465-14

Dai, Z., Fagherazzi, S., Mei, X., Chen, J., & Meng, Y. (2016). Linking the infilling of the North Branch in the Changjiang (Yangtze) estuary to anthropogenic activities from 1958 to 2013. *Marine Geology*, *379*, 1–12. https://doi.org/10.1016/j.margeo.2016.05.006

D'Alpaos, A., Carniello, L., & Rinaldo, A. (2013). Statistical mechanics of wind wave-induced erosion in shallow tidal basins: Inferences from the Venice Lagoon. *Geophysical Research Letters*, *40*(13), 3402–3407. https://doi.org/10.1002/grl.50666

D'Alpaos, A., Lanzoni, S., Marani, M., & Rinaldo, A. (2007). Landscape evolution in tidal embayments: Modeling the interplay of erosion, sedimentation, and vegetation dynamics. *Journal of Geophysical Research F: Earth Surface*, *112*(1). Retrieved from http://www.scopus.com/inward/record.url?eid=2-s2.0-34249739092&partnerID=40&md5=2ab44597de45d00ebe7091d9815acc5c

de Paiva, J. N. S., Walles, B., Ysebaert, T., & Bouma, T. J. (2018). Understanding the conditionality of ecosystem services: The effect of tidal flat morphology and oyster reef characteristics on sediment stabilization by oyster reefs. *Ecological Engineering*, *112*, 89–95. https://doi.org/10.1016/j.ecoleng.2017.12.020

Friedrichs, C. T. (2011). Tidal Flat Morphodynamics: A Synthesis. In E. Wolanski, & D. McLusky (Eds.), *Treatise on estuarine and coastal science* (pp. 137–170). Academic Press. https://doi.org/10.1016/b978-0-12-374711-2.00307-7

Friess, D. A., Rogers, K., Lovelock, C. E., Krauss, K. W., Hamilton, S. E., Lee, S. Y., et al. (2019). The state of the World's Mangrove Forests: Past, present, and future. *Annual Review of Environment and Resources*, *44*(1), 89–115. https://doi.org/10.1146/annurev-environ-101718-033302

Ganju, N. K., Defne, Z., Kirwan, M. L., Fagherazzi, S., D'Alpaos, A., & Carniello, L. (2017). Spatially integrative metrics reveal hidden vulnerability of microtidal salt marshes. *Nature Communications*, *8*. https://doi.org/10.1038/ncomms14156

Ge, Z., Cao, H., & Zhang, L. (2013). A process-based grid model for the simulation of range expansion of Spartina alterniflora on the coastal saltmarshes in the Yangtze Estuary. *Ecological Engineering*, *58*, 105–112. https://doi.org/10.1016/j.ecoleng.2013.06.024

Ge, Z., Wang, H., Cao, H., Zhao, B., Zhou, X., Peltola, H., et al. (2016). Responses of eastern Chinese coastal salt marshes to sea-level rise combined with vegetative and sedimentary processes. *Scientific Reports*, *6*. https://doi.org/10.1038/srep28466

Giosan, L., Syvitski, J., Constantinescu, S., & Day, J. (2014). Protect the world's deltas. *Nature*, *516*(7529), 31–33. https://doi.org/10.1038/516031a

Gray, A. J., Marshall, D. F., & Raybould, A. F. (1991). A Century of Evolution in Spartina anglica. In M. Begon, A. H. Fitter, & A. Macfadyen (Eds.), *Advances in Ecological Research* (Vol. *21*, pp. 1–62). Academic Press. https://doi.org/10.1016/S0065-2504(08)60096-3

Hu, Z. (2021). Data and model code for study: Mechanistic modelling of marsh seedling establishment provides a positive outlook for coastal wetland restoration under global climate change. *Zenodo*. https://doi.org/10.5281/zenodo.4916905

Hu, Z., Van Belzen, J., Van Der Wal, D., Balke, T., Wang, Z. B., Stive, M., & Bouma, T. J. (2015). Windows of opportunity for salt marsh vegetation establishment on bare tidal flats: The importance of temporal and spatial variability in hydrodynamic forcing. *Journal of Geophysical Research G: Biogeosciences*, *120*(7), 1450–1469. https://doi.org/10.1002/2014JG002870

Hu, Z., van der Wal, D., Cai, H., van Belzen, J., & Bouma, T. J. (2018). Dynamic equilibrium behaviour observed on two contrasting tidal flats from daily monitoring of bed-level changes. *Geomorphology*, *311*, 114–126. https://doi.org/10.1016/j.geomorph.2018.03.025

Hu, Z., Wang, Z. B., Zitman, T. J., Stive, M. J. F., & Bouma, T. J. (2015). Predicting long-term and short-term tidal flat morphodynamics using a dynamic equilibrium theory. *Journal of Geophysical Research-Earth Surface*, *120*(9), 1803–1823. https://doi.org/10.1002/2015JF003486

Kirwan, M. L., & Mudd, S. M. (2012). Response of salt-marsh carbon accumulation to climate change. *Nature*, *489*(7417), 550–553. https://doi.org/10.1038/nature11440

Kirwan, M. L., Temmerman, S., Skeehan, E. E., Guntenspergen, G. R., & Fagherazzi, S. (2016). Overestimation of marsh vulnerability to sea level rise. *Nature Climate Change*, *6*(3), 253–260. https://doi.org/10.1038/nclimate2909

Kirwan, M. L., Walters, D. C., Reay, W. G., & Carr, J. A. (2016). Sea level driven marsh expansion in a coupled model of marsh erosion and migration. *Geophysical Research Letters*, *43*(9), 4366–4373. https://doi.org/10.1002/2016GL068507

Ladd, C. J. T., Duggan-Edwards, M. F., Bouma, T. J., Pagès, J. F., & Skov, M. W. (2019). Sediment supply explains long-term and large-scale patterns in salt marsh lateral expansion and erosion. *Geophysical Research Letters*, *46*, 11178–11187. https://doi.org/10.1029/2019GL083315

Leonardi, N., Ganju, N. K., & Fagherazzi, S. (2015). A linear relationship between wave power and erosion determines salt-marsh resilience to violent storms and hurricanes. *Proceedings of the National Academy of Sciences*, *113*, 64–68. https://doi.org/10.1073/pnas.1510095112

Li, P., Yang, S. L., Milliman, J. D., Xu, K. H., Qin, W. H., Wu, C. S., et al. (2012). Spatial, temporal, and human-induced variations in suspended sediment concentration in the surface waters of the Yangtze Estuary and adjacent Coastal Areas. *Estuaries and Coasts*, *35*(5), 1316–1327. https://doi.org/10.1007/s12237-012-9523-x

Liu, X. J., Gao, S., & Wang, Y. P. (2011). Modeling profile shape evolution for accreting tidal flats composed of mud and sand: A case study of the central Jiangsu coast, China. *Continental Shelf Research*, *31*(16), 1750–1760. https://doi.org/10.1016/j.csr.2011.08.002

Maan, D. C., Van, P., Wang, Z. B., & De, V. (2015). Do intertidal flats ever reach equilibrium? *Journal of Geophysical Research F: Earth Surface*, *120*(11), 2406–2436. https://doi.org/10.1002/2014JF003311

Marani, M., D'Alpaos, A., Lanzoni, S., & Santalucia, M. (2011). Understanding and predicting wave erosion of marsh edges. *Geophysical Research Letters*, *38*(21). https://doi.org/10.1029/2011gl048995

Mariotti, G., & Canestrelli, A. (2017). Long-term morphodynamics of muddy backbarrier basins: Fill in or empty out? *Water Resources Research*, *53*(8), 7029–7054. https://doi.org/10.1002/2017WR020461

Mariotti, G., & Fagherazzi, S. (2013). Critical width of tidal flats triggers marsh collapse in the absence of sea-level rise. *Proceedings of the National Academy of Sciences*, *110*(14), 5353–5356. https://doi.org/10.1073/pnas.1219600110

Mcleod, E., Chmura, G. L., Bouillon, S., Salm, R., Bjork, M., Duarte, C. M., et al. (2011). A blueprint for blue carbon: Toward an improved understanding of the role of vegetated coastal habitats in sequestering CO_2. *Frontiers in Ecology and the Environment*, *9*(10), 552–560. https://doi.org/10.1890/110004

Nittrouer, J. A., Best, J. L., Brantley, C., Cash, R. W., Czapiga, M., Kumar, P., & Parker, G. (2012). Mitigating land loss in coastal Louisiana by controlled diversion of Mississippi River sand. *Nature Geoscience*, *5*(8), 534–537. https://doi.org/10.1038/NGEO1525

Parkinson, R. W., Craft, C., DeLaune, R. D., Donoghue, J. F., Kearney, M., Meeder, J. F., et al. (2017). Marsh vulnerability to sea-level rise. *Nature Climate Change*, *7*(11), 756–756. https://doi.org/10.1038/nclimate3424

Roberts, W., Le Hir, P., & Whitehouse, R. J. S. (2000). Investigation using simple mathematical models of the effect of tidal currents and waves on the profile shape of intertidal mudflats. *Continental Shelf Research*, *20*(10–11), 1079–1097. https://doi.org/10.1016/s0278-4343(00)00013-3

Schuerch, M., Spencer, T., Temmerman, S., Kirwan, M. L., Wolff, C., Lincke, D., et al. (2018). Future response of global coastal wetlands to sea-level rise. *Nature*, *561*(7722), 231, 234–+. https://doi.org/10.1038/s41586-018-0476-5

Schwarz, C., Gourgue, O., van Belzen, J., Zhu, Z., Bouma, T. J., van de Koppel, J., et al. (2018). Self-organization of a biogeomorphic landscape controlled by plant life-history traits. *Nature Geoscience*, *1*, 672–677. https://doi.org/10.1038/s41561-018-0180-y

Singh Chauhan, P. P. (2009). Autocyclic erosion in tidal marshes. *Geomorphology*, *110*(3–4), 45–57. https://doi.org/10.1016/j.geomorph.2009.03.016

Smith, J. M., Bryant, M. A., & Wamsley, T. V. (2016). Wetland buffers: Numerical modeling of wave dissipation by vegetation. *Earth Surface Processes and Landforms*, *41*(6), 847–854. https://doi.org/10.1002/esp.3904

Stive, M. J. F., De, S., Luijendijk, A. P., Aarninkhof, S. G. J., Van, G.-M., Van, T. D. V., et al. (2013). A new alternative to saving our beaches from sea-level rise: The sand engine. *Journal of Coastal Research*, *29*(5), 1001–1008. https://doi.org/10.2112/JCOASTRES-D-13-00070.1

Strong, D. R., & Ayres, D. R. (2013). Ecological and Evolutionary Misadventures of Spartina. *Annual Review of Ecology Evolution and Systematics*, *44*(1), 389–410. https://doi.org/10.1146/annurev-ecolsys-110512-135803

Suykerbuyk, W., Bouma, T. J., Govers, L. L., Giesen, K., de Jong, D. J., Herman, P., et al. (2015). Surviving in changing seascapes: Sediment dynamics as bottleneck for long-term seagrass presence. *Ecosystems*, *19*(2), 296–310. https://doi.org/10.1007/s10021-015-9932-3

Syvitski, J. P. M., Kettner, A. J., Overeem, I., Hutton, E. W. H., Hannon, M. T., Brakenridge, G. R., et al. (2009). Sinking deltas due to human activities. *Nature Geoscience*, *2*(10), 681–686. https://doi.org/10.1038/ngeo629

Temmerman, S., Meire, P., Bouma, T. J., Herman, P. M. J., Ysebaert, T., & De Vriend, H. J. (2013). Ecosystem-based coastal defence in the face of global change. *Nature*, *504*(7478), 79–83. https://doi.org/10.1038/nature12859

Thorne, K., MacDonald, G., Guntenspergen, G., Ambrose, R., Buffington, K., Dugger, B., et al. (2018). U.S. Pacific coastal wetland resilience and vulnerability to sea-level rise. *Science Advances*, *4*(2), eaao3270. https://doi.org/10.1126/sciadv.aao3270

van der Wal, D., Wielemaker-Van den Dool, A., & Herman, P. M. J. (2008). Spatial patterns, rates and mechanisms of saltmarsh cycles (Westerschelde, The Netherlands). *Estuarine, Coastal and Shelf Science*, *76*(2), 357–368. https://doi.org/10.1016/j.ecss.2007.07.017

van der Werf, J., Reinders, J., van Rooijen, A., Holzhauer, H., & Ysebaert, T. (2015). Evaluation of a tidal flat sediment nourishment as estuarine management measure. *Ocean & Coastal Management*, *114*, 77–87. https://doi.org/10.1016/j.ocecoaman.2015.06.006

van Loon-Steensma, J. M., Hu, Z., & Slim, P. A. (2016). Modelled Impact of vegetation heterogeneity and Salt-Marsh Zonation on Wave Damping. *Journal of Coastal Research*, *32*(2), 241–252. https://doi.org/10.2112/JCOASTRES-D-15-00095.1

Wang, C., & Temmerman, S. (2013). Does biogeomorphic feedback lead to abrupt shifts between alternative landscape states?: An empirical study on intertidal flats and marshes. *Journal of Geophysical Research-Earth Surface*, *118*(1), 229–240. https://doi.org/10.1029/2012JF002474

Wang, H., Ge, Z., Yuan, L., & Zhang, L. (2014). Evaluation of the combined threat from sea-level rise and sedimentation reduction to the coastal wetlands in the Yangtze Estuary, China. *Ecological Engineering*, *71*, 346–354. https://doi.org/10.1016/j.ecoleng.2014.07.058

Young, I. R., & Ribal, A. (2019). Multiplatform evaluation of global trends in wind speed and wave height. *Science*, *364*(6440), 548–552. https://doi.org/10.1126/science.aav9527

Young, I. R., Zieger, S., & Babanin, A. V. (2011). Global trends in wind speed and wave height. *Science*, *332*(6028), 451–455. https://doi.org/10.1126/science.1197219

Zhu, Z., Vuik, V., Visser, P. J., Soens, T., van Wesenbeeck, B., van de Koppel, J., et al. (2020). Historic storms and the hidden value of coastal wetlands for nature-based flood defence. *Nature Sustainability*, *1*, 853–862. https://doi.org/10.1038/s41893-020-0556-z

Zhu, Z., Zhang, L., Wang, N., Schwarz, C., & Ysebaert, T. (2012). Interactions between the range expansion of saltmarsh vegetation and hydrodynamic regimes in the Yangtze Estuary, China. *Estuarine, Coastal and Shelf Science*, *96*(1), 273–279. https://doi.org/10.1016/j.ecss.2011.11.027

References From the Supporting Information

Goldstein, E. B., Coco, G., & Plant, N. G. (2019). A review of machine learning applications to coastal sediment transport and morphodynamics. *Earth-Science Reviews*, *194*, 97–108. https://doi.org/10.1016/j.earscirev.2019.04.022

Oehler, F., Coco, G., Green, M. O., & Bryan, K. R. (2012). A data-driven approach to predict suspended-sediment reference concentration under non-breaking waves. *Continental Shelf Research*, *46*, 96–106. https://doi.org/10.1016/j.csr.2011.01.015

Yoon, H.-D., Cox, D. T., & Kim, M. (2013). Prediction of time-dependent sediment suspension in the surf zone using artificial neural network. *Coastal Engineering*, *71*, 78–86. https://doi.org/10.1016/j.coastaleng.2012.08.005

Zhu, Q., van, P., Wang, Z. B., & Yang, S. L. (2017). Bed-level changes on intertidal wetland in response to waves and tides: A case study from the Yangtze River Delta. *Marine Geology*, *385*, 160–172. https://doi.org/10.1016/j.margeo.2017.01.003